Title

Opioid system is necessary but not sufficient for antidepressive actions of ketamine in rodents

Journal

Proceedings of the National Academy of Sciences of the United States of America, 117(5)

ISSN

0027-8424

Authors

Klein, Matthew E
Chandra, Joshua
Sheriff, Salma
et al.

Publication Date

2020-02-04

DOI

10.1073/pnas.1916570117

Peer reviewed

Opioid system is necessary but not sufficient for antidepressive actions of ketamine in rodents

Matthew E. Klein[a,b,c,1], Joshua Chandra[b,c], Salma Sheriff[b,c], and Roberto Malinow[b,c,1]

[a]Department of Psychiatry, University of California San Diego (UCSD) School of Medicine, San Diego, CA 92093; [b]Department of Neurosciences, UCSD School of Medicine, San Diego, CA 92093; and [c]Section of Neurobiology, Division of Biology, UCSD, San Diego, CA 92093

Contributed by Roberto Malinow, November 29, 2019 (sent for review September 24, 2019; reviewed by Hailan Hu and Bo Li)

Slow response to the standard treatment for depression increases suffering and risk of suicide. Ketamine, an *N*-methyl-D-aspartate (NMDA) receptor antagonist, can rapidly alleviate depressive symptoms and reduce suicidality, possibly by decreasing hyperactivity in the lateral habenula (LHb) brain nucleus. Here we find that in a rat model of human depression, opioid antagonists abolish the ability of ketamine to reduce the depression-like behavioral and LHb hyperactive cellular phenotypes. However, activation of opiate receptors alone is not sufficient to produce ketamine-like effects, nor does ketamine mimic the hedonic effects of an opiate, indicating that the opioid system does not mediate the actions of ketamine but rather is permissive. Thus, ketamine does not act as an opiate but its effects require both NMDA and opiate receptor signaling, suggesting that interactions between these two neurotransmitter systems are necessary to achieve an antidepressant effect.

lateral habenula | ketamine | opioid system

Low-dose ketamine is being increasingly used in the treatment of acute suicidality and refractory depression (1, 2). The rapid therapeutic onset is particularly well suited for use in urgent settings, as standard treatments often require weeks to achieve clinical effects (3). Unlike other drugs currently used for depression treatment, ketamine displays high affinity for, and inhibits, the *N*-methyl-D-aspartate (NMDA) receptor (NMDAR; $K_i \sim 0.5$ μM) (4, 5). While NMDAR antagonists including APV and MK-801 produce short-lived antidepressant responses in preclinical studies, clinical studies have generally not demonstrated an antidepressant response of NMDAR-blocking agents, possibly due to different pharmacokinetics of the drugs (6, 7). Ketamine also inhibits other targets, albeit with significantly lower affinity [e.g., μ-opioid receptor, μOR; $K_i > 10$ μM (8)]. Ketamine analgesia, achieved with higher than antidepressive doses, is diminished by coadministration of μOR antagonists, suggesting that ketamine may have activity at both opiate and NMDA receptors at biologically relevant concentrations (9–13). It is thus unclear if the antidepressant effects of ketamine are mediated solely through NMDARs. Indeed, a recent small clinical study found that the antidepressant and antisuicidal effects of ketamine were blocked by the opioid antagonist naltrexone (refs. 14 and 15, but see refs. 16–19). Furthermore, opiates have long been clinically used for mood augmentation with ongoing clinical trials of novel formulations (20–23). The possibility that ketamine acts as an opiate has raised valid concerns among clinicians that could significantly impact its use (24).

The lateral habenula (LHb; coined the "disappointment center") is part of a midbrain circuit that inhibits dopamine neurons in the ventral tegmental area after punishment or absence of an expected reward (25, 26). These features are thought to be key in normal reinforcement learning (27). In animal models, excessive LHb activity contributes to a number of behaviors that mimic core aspects of human depression (28), and inhibiting the LHb reduces such behaviors in rodents (29–32) and can ameliorate human depression (33). Notably, systemic ketamine delivery in humans (34) or intrahabenular delivery in rodents reduces LHb activity and depression-like behaviors (35).

A well-characterized rodent model to study the circuitry and pharmacology of depression is provided by the congenitally learned helpless (cLH) rat. cLH animals have been inbred from Sprague–Dawley rats based on susceptibility to learned helplessness after inescapable shock training (36). Unlike the wild type (WT), cLH rats exhibit a helpless phenotype without prior exposure to stress, as demonstrated in the shuttle box or forced swim test (37). Consistent with its modeling maladaptive valence processing, cLH animals display abnormal reward responses like those observed in depressed patients (38–40). Furthermore, this line displays several depression-like symptoms (e.g., anhedonia, avolition, weight changes) (41) that improve with drugs (42–44) used to treat human depression, including ketamine (35).

Here we test if the effects of low-dose ketamine are mediated by the opioid system, using behavioral and cellular assays. Is the μOR necessary and sufficient for the effects of ketamine? We find that μOR activity is necessary for the effects of ketamine, but μOR activation is not by itself sufficient to produce ketamine-like effects. These results suggest that μORs permit, but do not directly transmit, the actions of ketamine.

Materials and Methods

Subjects. Male cLH and WT Sprague–Dawley rats, aged 3 to 4 wk for virus injection and aged 8 to 12 wk for behavioral studies, were kept on a 12/12-h, reverse-light/dark cycle (lights off 9 AM to 9 PM, lights on 9 PM to 9 AM).

Significance

Ketamine, an NMDA receptor antagonist, has generated intense excitement as a therapy for treatment-resistant depression. However, ketamine and its metabolites can act on a wide range of targets, including opioid receptors, which has raised concerns. Using behavioral and cellular assays in rodents, we find that blocking opioid function prevents the antidepressant-like effects of ketamine. However, in contrast to ketamine, administration of a μ-opioid agonist is hedonic and ineffective on anhedonia/avolition. Furthermore, ketamine's cellular actions are both mimicked and occluded by an NMDAR antagonist but not by a μ-opioid agonist. These results suggest that ketamine does not act as a μ-opioid agonist, but functional μ-opioid receptors are permissive for the antidepressant effects of ketamine.

Author contributions: M.E.K. and R.M. designed research; M.E.K., J.C., and S.S. performed research; M.E.K. and R.M. analyzed data; and M.E.K. and R.M. wrote the paper.

Reviewers: H.H., Zhejiang University; and B.L., Cold Spring Harbor Laboratory.

The authors declare no competing interest.

[1]To whom correspondence may be addressed. Email: meklein@ucsd.edu or rmalinow@ucsd.edu.

This article contains supporting information online at https://www.pnas.org/lookup/suppl/doi:10.1073/pnas.1916570117/-/DCSupplemental.

First published January 15, 2020.

Red filters were used for lighting during daytime care. All procedures involving animals were approved by the Institutional Animal Care and Use Committees of the University of California San Diego.

Drugs. Ketamine (Zoetis; 15 mg/kg, intraperitoneally [i.p.]), morphine (Hospira; 10 mg/kg, subcutaneously [s.c.]), and naltrexone hydrochloride (Tocris; 1 mg/kg, s.c.) were dissolved in 0.9% saline for injection. Mice in the control group were injected with 0.9% saline. All doses were calculated according to the base weight of the drug. Drugs for slice experiments were as follows: 2,3-dioxo-6-nitro-1,2,3,4-tetrahydrobenzo[*f*]quinoxaline-7-sulfonamide (NBQX; Tocris; 10 μM), D-(−)-2-amino-5-phosphonopentanoic acid (D-APV; Tocris; 25 μM), tetrodotoxin (TTX; Tocris; 1 μM), CTAP ([d-Phe-Cys-Tyr-d-Trp-Arg-Thr-Pen-Thr-NH2]; Tocris; 100 nM), [D-Ala^2, NMe-Phe^4, Gly-ol^5]-enkephalin (DAMGO; Tocris; 1 μM), ketamine (Tocris; 10 μM), naltrexone (Tocris; 1 μM), and morphine (Hospira; 0.9 μM).

Forced Swim Test. Rats were subjected to a 1-d modified forced swim test (mFST) as cLH animals do not require a "pretest" swim day to display immobility behavior (32). Subjects were brought up from the vivarium during the dark cycle and allowed to acclimate in a quiet, dark room for 1 h before drug injection and testing. Rats were placed in a clear cylinder filled with 12″ of 35 °C temperature water and observed by video camera for 15 min, upon which the test was stopped. Drug injections were performed as described in the main text.

Analysis of mFST movies was performed using the open-source Bonsai software package as described previously (45). Movies were cropped to include the subject and automatically thresholded into a binary image where the subject was represented as pixels with a value of 1 and background pixels as 0. Identical threshold parameters were used for each movie. Subject movement was quantified as standard motion pixels [SMPs (46)]. Subsequent frames of the thresholded movie were subtracted from each other and movement was determined by the number of pixels that changed. The resulting mobility over time (15 min) graph was normalized for each animal by setting the minimum to 0 and the maximum to 1. Percent immobility for the session was determined by calculating the number of SMP values below a predetermined threshold that remained consistent across all subjects. Restricting analysis to the last 4 min of testing, rather than the full 15 min, did not significantly alter conclusions. Experiments with vehicle and ketamine were interspersed across testing sessions and results were pooled for graphing and statistical comparisons.

Conditioned Place Preference. Conditioned place preference (CPP) took place over the course of 6 d. On the first day, rats were placed into a box divided into two chambers by a metal divider. The two chambers were decorated uniquely with both tactile and visual cues. The rats could freely roam for 15 min, and their position in the chambers was monitored by video camera, after which a side preference for each rat was calculated depending on which of the two chambers they preferred. Most rats did not appear to have a significant preference on the first day. On the subsequent 4 d, rats were either injected with morphine or ketamine and detained in their nonfavored side. On the sixth, and final, day, rats were injected with saline and again allowed to roam freely across both sides of the chamber. Place preference is reported as the absolute time the rat spends on the conditioned side the first day and the final day.

Progressive Ratio. Rats were food-restricted to 90% of their body weight following protocols established by the Institutional Animal Care and Use Committees of the University of California, San Diego. Once at testing weight, rats were trained in a Pavlovian task to associate the illumination of a magazine light with availability of a reward at the delivery port (20 to 30 μL 7% sucrose). Most subjects had >100 port entries during the first training session, and were continued on to fixed ratio (FR1) training. During the 30-min FR1 training sessions, subjects could press a lever, once a light indicated reward availability, to receive a sucrose reward from the port. Once subjects achieved >60 lever presses in a session, they were given 1 d of FR5 training to stabilize lever-pressing behavior. Subjects were then allowed to rest in their home vivarium for several days before starting the progressive ratio (PR) schedule. The PR schedule started with an assessment of the baseline number of lever presses a subject would perform to receive a sucrose reward. Sucrose reinforcements could be earned with the following number of presses: 1, 2, 3, 4, 5, 6, 7, 8, 9, 10, 12, 14, 16, 18, 20, 22, 24, 28, 32, 36, 40, 44, 48, 52, 56, 64, 72, 80, and 88. The final ratio achieved represented the breakpoint value. The next day, rats were treated as described in the text and the breakpoint was reassessed 2 h post treatment as well 1 and 7 d post treatment.

Surgery. Rodents were anesthetized with isoflurane for stereotaxic injection of an adeno-associated virus (AAV) expressing jGCaMP7f (AddGene; pGP-AAV-syn-jGCaMP7f-WPRE; AAV8) bilaterally into the LHb (anterior–posterior, −3.2 mm; medial–lateral, ±0.5 mm; dorsal–ventral, −4.85 to −5.0 mm). A total of 0.5 to 1.0 μL virus was injected over an 8- to 10-min period. At the end of the injection, the pipet remained at the site for 5 min to allow for diffusion of the virus into the surrounding tissue. Rats were injected with 5 mg carprofen (a nonsteroidal antiinflammatory drug) per kg body weight after surgery.

Calcium Imaging. Three weeks after viral injection, rats were anesthetized with isoflurane before decapitation and brain removal. Brains were chilled in ice-cold dissection buffer (215 mM sucrose, 20 mM glucose, 26 mM $NaHCO_3$, 4 mM $MgCl_2$, 4 mM $MgSO_4$, 1.6 mM NaH_2PO_4, 1 mM $CaCl_2$, and 2.5 mM KCl), gassed with 95%/5% O_2/CO_2 (carbogen), and cut into 300-μm-thick coronal slices through the LHb. Slices were transferred to 35 °C in a 50%/50% mixture of dissection buffer and artificial cerebrospinal fluid (ACSF) (124 mM NaCl, 26 mM $NaHCO_3$, 10 mM glucose, 2.5 mM KCl, 1 mM NaH_2PO_4, 4 mM $CaCl_2$, and 2 mM $MgCl_2$) and gassed with carbogen for 30 min. After an additional 30 min of recovery at room temperature, slices were transferred to room-temperature ACSF.

Acute LHb slices were imaged on a Prairie Labs 2p system, using Prairie View software and a Chameleon laser tuned to 980 nm. Regions with jGCaMP7f expression in the LHb were identified and 80 frames at 1.2 Hz (66 s total) were acquired. Two or three separate movies were acquired for each slice imaging session, a baseline, followed by one or two drug conditions. Each movie was separated by 15 min to permit drug penetration. For some experiments, two baseline movies were recorded 15 min apart to measure the baseline level of change in the absence of drugs. Vehicle experiments were interspersed among imaging sessions and the average baseline value across all experimental sessions was reused for graphing and statistical comparisons. Drug effect quantified as ratio of fluorescence intensity after drug application divided by intensity during baseline period. A ratio of 1 indicates no change; a ratio below 1 indicates the drug reduced activity.

Analysis. Calcium imaging analysis was performed using FIJI (ImageJ) and MATLAB. The movies for each slice were concatenated, registered (linear stack alignment with SIFT) in FIJI, and divided by the average projection across time image to create a $\Delta F/F$ movie. Segmentation of neuronal somas was performed automatically in MATLAB using the Calcium Signal Extract toolbox (Stephan Meyer, GitHub), and intensity over time was measured for each region of interest (ROI).

To exclude ROIs with constant decrease or increase, ROI $\Delta F/F$ intensity traces were detrended (MATLAB), and traces displaying less than 20% change over baseline were excluded. The rest of the analysis was performed on the nondetrended ROI $\Delta F/F$ traces encompassing baseline and drug treatment images. These traces were normalized by setting the lowest value of the 5-point moving average to 0 and the maximum intensity to 1. For each $\Delta F/F$ trace, the mean values during baseline and during drug treatment were calculated, and the ratio of mean activity in drug condition over baseline was calculated for each neuron. In the figure legends for imaging experiments, N/N' indicates the number of neurons (N) and number of animals (N'). For behavioral experiments, N is the number of animals.

Materials and Data Availability. All experimental procedures and data from this study are provided in the main text and *SI Appendix*. All rat strains and plasmids used in the study are available upon request, or can be obtained from Addgene (https://www.addgene.org/) by qualified researchers for their own use.

Results

An Antidepressant Dose of Ketamine Reduces LHb Cellular Hyperactivity. To dissect the cellular and behavioral effects of ketamine, we used congenitally learned helpless rats (cLH), which model some behaviors displayed in human depression (see above). To examine behavioral effects, we used a modified forced swim test (see *Materials and Methods* for details) (Fig. 1A_1). In this test, immobility is thought to model human maladaptive coping, as an animal stops escape movements in a hostile environment (47–49). In support of this view, cLH animals displayed more immobility than WT rats in the mFST (Fig. 1 A_2 and A_3).

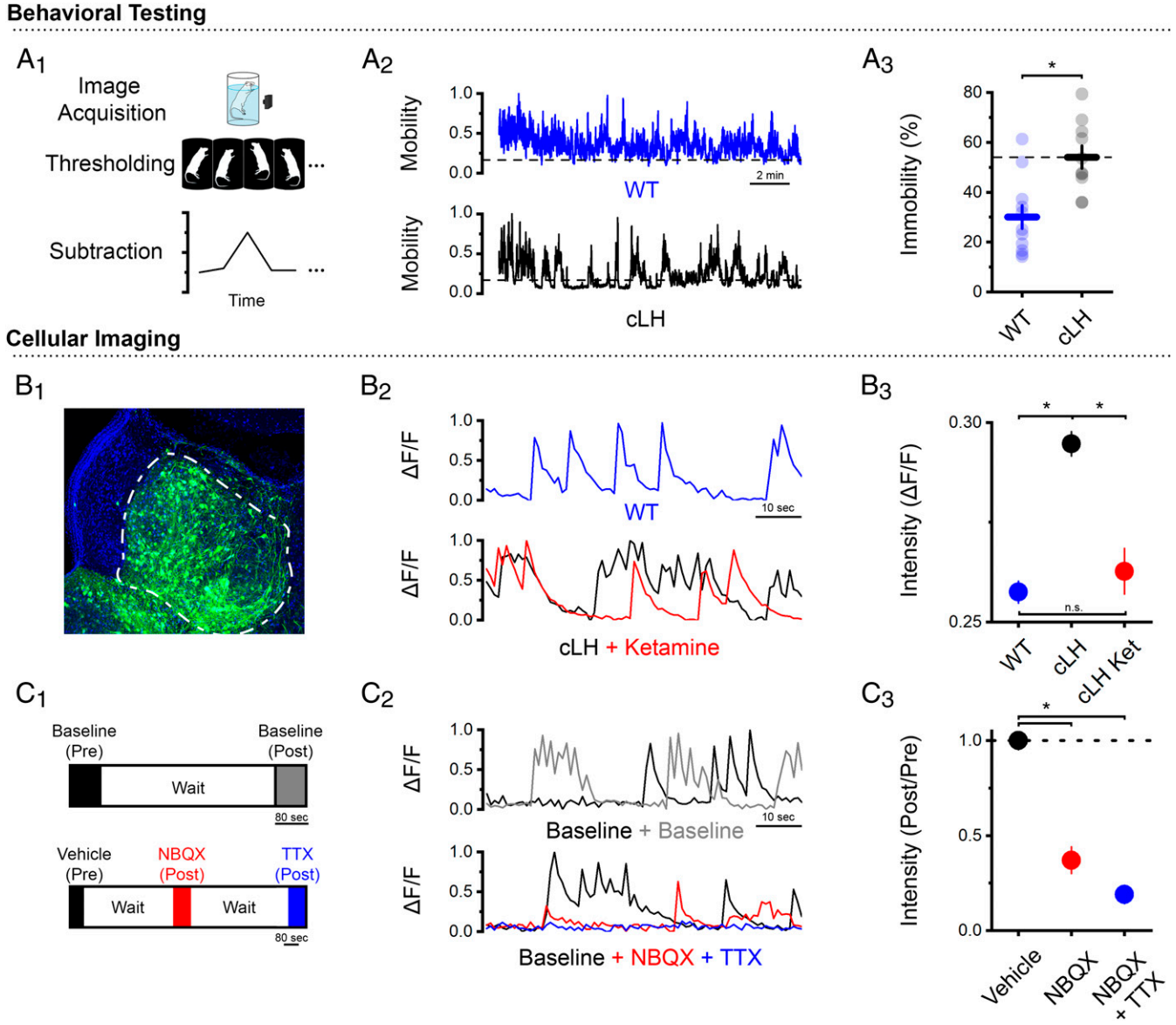

Fig. 1. Performance in the mFST is correlated with LHb cellular activity. (A_1) Schema depicting mFST. (A_2) Example rat movement over time, for indicated genotypes, in the mFST. Time spent below mobility threshold (dashed line) is immobility. (A_3) Summary data for mFST performance for indicated genotypes; horizontal bars, means ± SEM; circles, individual rat values; dashed line, cLH mean; here and throughout for immobility summary graphs. cLH animals were significantly more immobile than WT animals (% time immobile: cLH = 54 ± 5%, N = 11; WT = 30 ± 4%, N = 11; *P < 0.005, unpaired Student's t test). (B_1) Example 2-photon image of LHb acute slice; neurons expressing jGCamP7f. LHb demarcated by dashed line. (B_2) Example intensity ($\Delta F/F$) over time of individual LHb slice neurons from indicated genotypes and experimental conditions. (B_3) cLH tissue slice LHb neurons are more active than WT tissue neurons. Ketamine (10 μM, 15 min) reduces cLH activity to WT levels. Circles, mean ($\Delta F/F$) ± SEM. WT = 0.26 ± 0.002, N = 1,184/13 (cells/animals; here and throughout); cLH = 0.29 ± 0.003, N = 942/12; cLH+ketamine = 0.26 ± 0.006, N = 350/5. Difference in the means (F(2, 2,473) = 32, P < 0.005, one-way ANOVA; WT vs. cLH, and cLH vs. cLH ketamine, *P < 0.005; WT vs. cLH ketamine, P > 0.05, nonsignificant [n.s.]; Tukey posthoc test). (C_1) Calcium imaging experimental design comparing no treatment (*Top*) and drug treatments (*Bottom*). After letting the slice acclimate to the recording chamber for 5 min, an initial (pre) movie was acquired (80 frames, 1.2 Hz). Drug was then added to the perfusate and allowed to wash in for 15 min before a second movie was acquired. In some experiments a second drug was then added and a third movie was acquired, again after a 15 min washing in period. (C_2) Example calcium signals ($\Delta F/F$) over time of single LHb slice neurons from cLH slices for indicated experimental conditions. (C_3) Effect of indicated drugs (mean $\Delta F/F$ after drug divided by $\Delta F/F$ during baseline for neurons from cLH slices). A ratio of 1 indicates no change; a ratio below 1 indicates the drug reduced activity. Circles, mean ($\Delta F/F$) ± SEM; dashed line, baseline mean value; here and throughout for summary calcium signal graphs. Vehicle = 1.04 ± 0.05, N = 177/3; NBQX (10 μM) = 0.37 ± 0.07, N = 44/1; NBQX (10 μM) + TTX (1 μM) = 0.20 ± 0.04, N = 31/1. Difference in the means (F(2,249) = 36, P < 0.005, one-way ANOVA; vehicle vs. NBQX, and vehicle vs. NBQX+TTX, *P < 0.005; Tukey posthoc test).

To correlate LHb activity with performance in the mFST, we used calcium imaging in ex vivo brain slices containing the LHb. cLH and WT rats were injected bilaterally into the LHb with a virus (AAV) driving expression of the genetically encoded calcium indicator jGCaMP7f. Three weeks after such injections, which permitted expression of jGCaMP7f, acute coronal sections containing the LHb were prepared (Fig. 1B_1). These ex vivo slices were placed in a chamber perfused with ACSF and imaged using 2-photon microscopy. Using this technique, which allowed for rapid screening of pharmacological agents, we monitored the

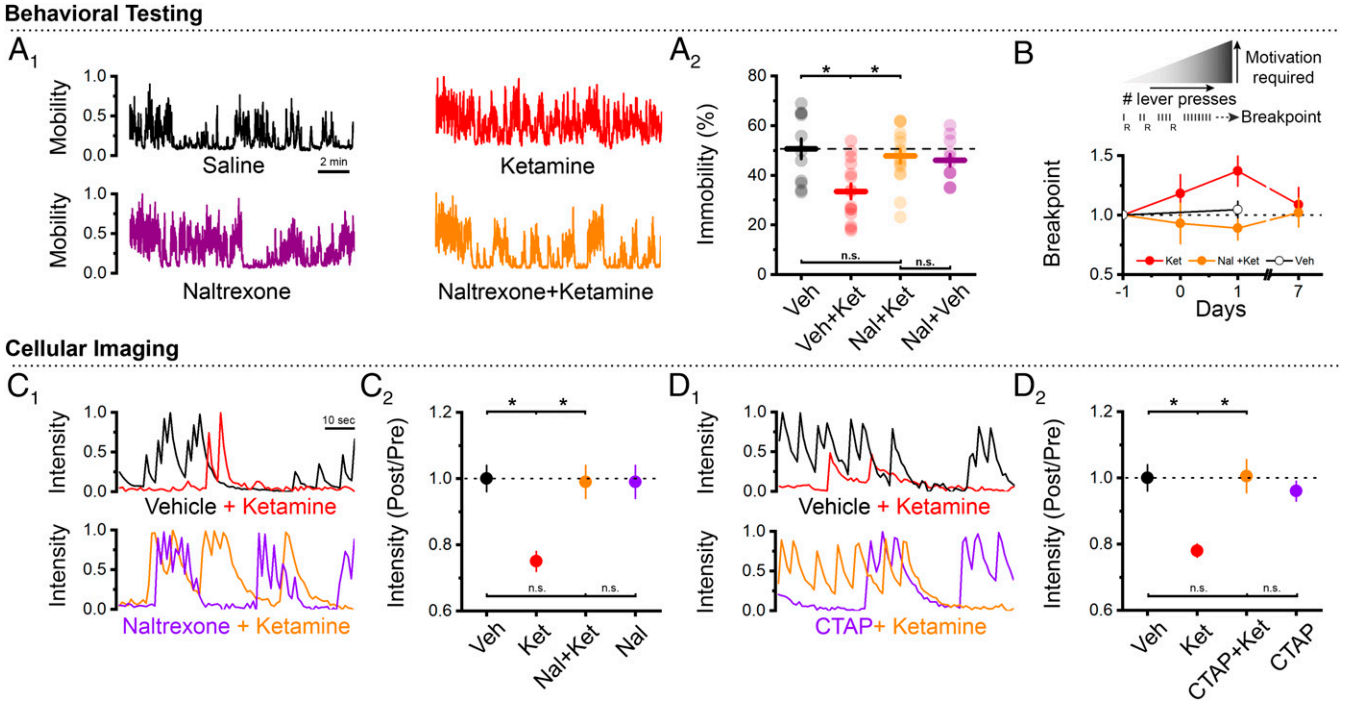

Fig. 2. Inhibition of μ-opioid receptors opposes the behavioral and cellular effects of ketamine. (A_1) Example cLH rat mFST mobility, for indicated drug conditions. (A_2) Immobility summary graph for indicated drug conditions. Vehicle = 50 ± 5%, N = 11; ketamine = 34 ± 3%, N = 15; naltrexone+ketamine = 48 ± 3%, N = 16; naltrexone = 46 ± 2%, N = 12. A 2-way ANOVA revealed a statistically significant interaction of pretreatment (naltrexone) × treatment (ketamine) (F(1, 50) = 9.73, P < 0.005) on immobility in the mFST. Vehicle vs. vehicle+ketamine, vehicle+ketamine vs. naltrexone+ketamine, *P < 0.05; vehicle vs. naltrexone+ketamine, naltrexone+ketamine vs. naltrexone+vehicle, P > 0.05, nonsignificant (n.s.); Tukey posthoc test. (*B*, *Top*) Schema of progressive ratio test. (*B*, *Bottom*) Mean (± SEM) normalized breakpoint summary data for indicated treatments and days: ketamine, 1, 1.2 ± 0.2, 1.4 ± 0.1, 1.1 ± 0.1, N=6; naltrexone+ketamine, 1, 0.9 ± 0.2, 0.9 ± 0.1, 1.0 ± 0.1, N = 7; vehicle, 1, 1.0 ± 0.1, N = 13. Difference in the population means between ketamine and naltrexone+ketamine (F(2,30) = 5.79, P < 0.05), 2-way ANOVA. (C_1) Example intensity (ΔF/F) over time graphs of single LHb slice neurons for indicated conditions. (C_2) Calcium signal summary graph for indicated conditions. Vehicle = 1.00 ± 0.04, N = 208/9; ketamine = 0.75 ± 0.03, N = 178/6; naltrexone+ketamine = 0.99 ± 0.05, N = 176/5; naltrexone = 0.99 ± 0.05, N = 144/4. A 2-way ANOVA revealed a statistically significant interaction of pretreatment (naltrexone) × treatment (ketamine) (F(1,702) = 11.17, P < 0.005) on LHb neuronal activity. Vehicle vs. ketamine, ketamine vs. naltrexone+ketamine, *P < 0.05; vehicle vs. naltrexone+ketamine, vehicle vs. naltrexone, naltrexone+ketamine vs. naltrexone, P > 0.05 (n.s.); Tukey posthoc test. (D_1) Example intensity (ΔF/F) over time graphs of single LHb slice neurons for indicated conditions. (D_2) Same as C_2; vehicle = 1.00 ± 0.04, N = 208/9; ketamine = 0.78 ± 0.02, N = 235/8; CTAP+ketamine = 1.01 ± 0.05, N = 85/4; CTAP = 0.96 ± 0.03, N = 181/7. Two-way ANOVA revealed a statistically significant interaction of pretreatment (CTAP) × treatment (ketamine) (F(1,705) = 11.17, P < 0.005) on LHB neuronal activity. Vehicle vs. ketamine, ketamine vs. CTAP+ketamine, *P < 0.05; vehicle vs. CTAP+ketamine, vehicle vs. CTAP, CTAP+ketamine vs. CTAP, P > 0.05 (n.s.); Tukey posthoc test.

changes in fluorescence, reflecting changes in neuronal firing, simultaneously in dozens of independently active neurons in each slice (see *Materials and Methods* for details). With this method, we confirmed that spontaneous neuronal activity in cLH tissue was significantly higher than that in WT tissue and reduced to WT levels by addition of 10 μM ketamine (35) (Fig. 1 B_2 and B_3). The duration of a bout of activity was significantly longer in cLH neurons than in WT neurons (*SI Appendix*, Fig. S1 *A* and B_1).

In a set of control experiments, imaging the activity of neurons during 66-s epochs separated by 15 min showed that, on average, neural firing did not change appreciably during this imaging period (Fig. 1*C*). However, activity was reduced by bath application of the AMPA (α-amino-3-hydroxy-5-methyl-4-isoxazolepropionic acid) receptor antagonist NBQX and further by subsequent application of the voltage-gated sodium channel antagonist TTX (Fig. 1 C_2 and C_3). These results indicate that the activity of neurons in these slices is at least in part driven by glutamatergic synaptic activity and reflects neuronal action potentials.

Antidepressant Effect of Ketamine Is Blocked by Naltrexone. Recent clinical work suggests that naltrexone, which blocks opioid receptors (K_i 1 nM for μ-opioid receptors and 4 nM for κ-opioid receptors), can interfere with the efficacy of ketamine (14, 15), although this finding was not supported by subsequent studies (16, 17, 19). To test if naltrexone blocks the antidepressant effects of ketamine, we employed 2 behavioral tests commonly used to measure anhedonia and motivation in rodent models.

First, the mFST was used to measure the interaction between ketamine and naltrexone on immobility using a 2-by-2 factorial design (Fig. 2A_1). Systemic injection of racemic ketamine 2 h before testing significantly reduced immobility in cLH animals compared with treatment with vehicle, consistent with an antidepressant effect. To test if opioid receptor activity is required, we administered systemically (s.c. injection, 1 mg/kg) naltrexone 1 h before ketamine and subsequently tested the animals (50). Pretreatment with naltrexone abolished the effects of subsequent ketamine treatment on immobility such that cLH animals treated with ketamine and naltrexone behaved as vehicle-treated animals. Naltrexone alone had no significant effect on immobility (Fig. 2A_2).

Next, cLH rats were trained on a PR task (PRT), where a lever must be pressed an increasing number of times to receive a sucrose reward (*Materials and Methods* and Fig. 2*B*). The breakpoint, the maximum number of lever presses before a rat stops the task, is used as a measure of motivation (45). In this schema, rats modeling the depressive-like symptoms of amotivation and avolition will stop at a lower breakpoint, and this metric can be improved by antidepressant treatment (51). The test could be administered consecutively (every few days) with no significant change in breakpoint. However, a single dose of ketamine administered to cLH rats

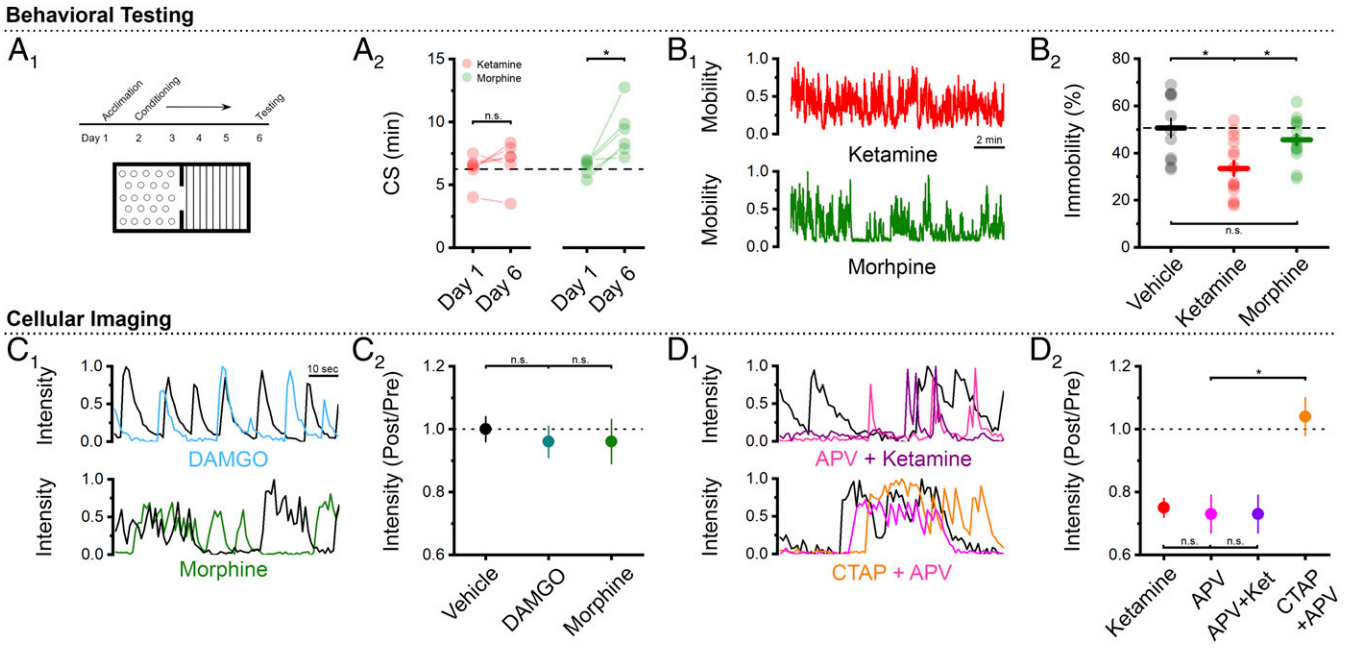

Fig. 3. Activation of μ-opioid receptors does not mimic the behavioral and cellular effects of ketamine in cLH animals. (A_1) Experimental schema of conditioned place preference (CPP) test. (A_2) Summary data for CPP test for indicated days and drugs, given after day 1 data collected. Circles, individual rats; dashed line, ketamine day 1 mean. Time spent in conditioned side (CS); ketamine, 15 mg/kg, ip; day 1, 6.2 ± 0.5 vs. day 6, 6.8 ± 0.7, $P > 0.05$ nonsignificant (n.s.); morphine, 10 mg/kg, sc; day 1, 6.4 ± 0.3; day 6, 9.2±0.8, $*P < 0.05$, Student's paired t test. (B_1) Example cLH rat mFST mobility, for indicated drug conditions. (B_2) Immobility summary graph for indicated conditions. Vehicle = 50 ± 5%, $N = 11$; ketamine = 34 ± 3%, $N = 15$; morhphine = 45 ± 2.3%, $N = 15$. Difference in the means ($F(2,38) = 6.6$, $P < 0.005$, one-way ANOVA); vehicle vs. ketamine, and ketamine vs. morphine, $*P < 0.05$; vehicle vs. morphine, $P > 0.05$ (n.s.); Tukey posthoc test. (C_1) Example intensity ($\Delta F/F$) over time graphs of single LHb slice neurons for indicated conditions; black, before drug. (C_2) Calcium signal summary graph for indicated conditions. Vehicle = 1.00 ± 0.04, $N = 208/9$; DAMGO = 0.96 ± 0.05, $N = 149/4$; morphine = 0.96 ± 0.07, $N = 73/3$. Difference in the means ($F(2,427) = 0.37$, $P > 0.05$, one-way ANOVA); vehicle vs. DAMGO, vehicle vs. morphine, DAMGO vs. morphine, $P > 0.05$ (n.s.); Tukey posthoc test. (D_1) Same as C_1, for indicated conditions; black, before drug. (D_2) Same as C_2, for indicated drugs. Ketamine = 0.75 ± 0.03, $N = 178/6$; APV = 0.73 ± 0.06, $N = 80/3$; APV+ketamine = 0.74 ± 0.06, $N = 56/3$; CTAP+APV = 1.04 ± 0.08, $N = 62/4$. Ketamine data reproduced from Fig. 2C_2. Difference in the means ($F(3,438) = 7.51$, $P < 0.05$, one-way ANOVA); APV vs. CTAP+APV, $*P < 0.05$; ketamine vs. APV, ketamine vs. APV+ketamine, and APV vs. AVP+ketamine, $P > 0.05$ (n.s.); Tukey posthoc test.

acutely increased the breakpoint, with maximal effect 1 d post treatment, and declined to baseline by 7 d post treatment. If naltrexone was coadministered with ketamine, no significant difference in breakpoint was observed in any of the days following treatment (Fig. 2*B*). Therefore, a subanesthetic dose of ketamine was able to rapidly improve cLH performance in two behavioral tests, and these effects were completely blocked by coadministration of the opiate antagonist naltrexone.

Ketamine Requires Intact μ-Opioid Receptor Signaling to Reduce LHb Hyperactivity. As naltrexone completely abolished the ability of ketamine to enhance the performance of rodents in both the mFST and PRT (Fig. 2 *A* and *B*), we sought to investigate the role of opiate signaling in the cellular actions of ketamine in the LHb of cLH animals. Compared with vehicle treatment, addition of ketamine (10 μM) to the perfusate acutely reduced cellular activity within 15 min (Fig. 2C_1 and *SI Appendix*, Fig. S1*C*). Ketamine appeared to preferentially reduce activity in neurons with greater burst-like baseline activity, while no such bias was observed in vehicle-treated neurons (*SI Appendix*, Fig. S1 B_2 and B_3). Naltrexone completely blocked the effects of ketamine, as addition of ketamine following naltrexone did not result in decreased LHb activity. Finally, addition of naltrexone alone to the perfusate did not alter LHb activity (Fig. 2C_2). As naltrexone antagonizes multiple classes of opioid receptors (50), we repeated our imaging experiments with the specific μOR antagonist CTAP (52). Similar to our previous results with naltrexone, CTAP completely abolished the effects of ketamine on LHb cellular hyperactivity, without having an effect when given alone (Fig. 2 D_1 and D_2). Together, these results demonstrate opioid receptors, and μOR in particular, are necessary for the rapid effects of ketamine at the behavioral and cellular levels, respectively.

A Hedonic Dose of Morphine Does Not Mimic Behavioral or Cellular Effects of Ketamine. Ketamine does display activity at opiate receptors, albeit at orders of magnitude less than NMDAR, and ketamine can be a drug of abuse, implying hedonic properties at a sufficiently high dose. To test for hedonic properties of an antidepressant dose of ketamine, we used the conditioned place preference test (*Materials and Methods* and Fig. 3A_1). This test determines if an animal prefers a compartment, of a two-compartment box, in which the animal previously received a drug (either morphine or ketamine at the doses used above). As expected, animals injected with morphine displayed place preference. However, animals injected with ketamine displayed no place preference (Fig. 3A_2). These results indicate that ketamine, at an antidepressant dose, did not produce hedonic behavior in the cLH rats.

As demonstrated in the previous experiments, a single, subanesthetic, nonhedonic dose of ketamine resulted in rapid effects on both behavioral and cellular activity. In contrast, a single hedonic dose of morphine (10 mg/kg, s.c.) did not mimic the effects of ketamine, demonstrating no effect on cLH performance in the mFST (Fig. 3 B_1 and B_2). Consistent with the lack of effect in the mFST, morphine application produced no significant effect in cellular activity of LHb slices (Fig. 3C_1). Additionally, activation of μORs by the specific agonist DAMGO had no effect on LHb activity (Fig. 3C_2). These results indicate that functional μORs are required for the cellular effects of ketamine in the LHb but that activation of μORs does not mimic the cellular effects of ketamine in the LHb.

Ketamine Acts on NMDARs to Reduce LHb Cellular Hyperactivity. Ketamine is a high-affinity antagonist of NMDAR (though its metabolites may have other properties), and this mechanism has been postulated to account for its antidepressant effect (1). To test if ketamine acts on NMDARs in the LHb, we noted that application of the specific NMDAR antagonist APV decreased LHb activity to a similar degree as ketamine (Fig. 3 D_1 and D_2). Furthermore, addition of ketamine after APV did not result in a further decrease in activity, demonstrating that APV mimics and prevents further effects of ketamine (Fig. 3 D_1 and D_2). This occlusion is not likely explained by reaching a floor of LHb activity, as previous experiments with NBQX and TTX resulted in even lower cellular activity (Fig. 1C_3). Similar to our observation with ketamine, the addition of CTAP into the perfusate completely blocked the effects of APV on LHb activity (Fig. 3 D_1 and D_2). These results indicate that ketamine reduces neuronal activity in cLH LHb slices by blocking NMDARs.

In sum, the behavioral results suggest that opioid receptor activity is necessary but μOR activation (at a dose that is able to produce a hedonic effect) is not sufficient for the effects of ketamine in a rodent model of human depression. At the cellular level, both μOR and NMDARs are required but μOR activation is not sufficient to produce the effect of ketamine on LHb hyperactivity.

Discussion

Here we use rodents to test the hypothesis that ketamine acts on opioid receptors to achieve its antidepressive effects. In our behavioral studies, we confirm that cLH animals display immobility and amotivation, behaviors thought to model human hopelessness. We find that ketamine administration rapidly improves these behaviors, and that these beneficial effects are blocked by naltrexone in multiple assays. Together, our results indicate that functional opioid receptors are required for ketamine to produce antidepressive-like behavioral effects in rodents. However, it does not appear that ketamine is directly acting on opiate receptors to produce these effects, as activation of μOR by morphine, sufficient to induce a hedonic response, did not mimic the rapid antidepressive-like effects of ketamine. Nor did it appear that ketamine, at an antidepressant dose, had a hedonic effect typically associated with μOR activation. Therefore, at least in rodents, low-dose ketamine does not have the same behavioral effects as μOR activation.

In our cellular studies, we focused on activity of neurons in the LHb, as hyperactivity of this region is thought to contribute to depression (34, 53), and normalization of this hyperactivity may be beneficial in treating depression (54). Furthermore, the LHb not only receives inputs from many opioid-sensitive brain regions but also contains a high density of μORs that can be directly modulated by opioids (55–57). Using a brain slice imaging method, we confirmed that LHb neurons from cLH animals display hyperactivity, when compared with neurons from WT animals, and were reduced to the activity level of WT animals by ketamine (35). As with the behavioral studies, this cellular effect of ketamine was blocked by naltrexone as well as by CTAP, indicating an intact μOR system is required for these effects. However, activation of μORs with a specific agonist failed to reduce LHb neuronal activity. Thus, in the results from our studies of LHb cellular activity, ketamine does not appear to act as a μOR agonist, though we cannot exclude the possibility that ketamine may be activating μORs in a manner that does not produce CPP or a hedonic effect. Our observation that the effects of the specific NMDA antagonist APV are also blocked by CTAP suggests that some activity of μOR is necessary for NMDAR antagonism, or the effects of NMDAR antagonism, as APV has no known action on μOR. It may be that this tonic action of μOR alters the biophysical properties of NMDAR to gate antagonism of both ketamine and APV. Therefore, the most direct interpretation of our results is that ketamine, at an antidepressive dose, is not mediating its behavioral or cellular effects by directly activating μOR. Rather, some level of μOR activity appears permissive as multiple lines of evidence with opioid antagonists do demonstrate the necessity of intact μOR signaling for ketamine to produce its rapid antidepressant response.

How then can μOR gate the response of ketamine? Indeed, there is a rich body of literature describing multiple interactions between these two signaling systems (58). Pain research studies, using ketamine at higher than antidepressive doses, suggest both direct and indirect interactions between ketamine and opioid receptors (1, 13, 59). At the electrophysiological level, NMDAR activation can be modulated by actions of opioid receptors (60–63). And, in some brain regions (including the habenula), NMDARs and opioid receptors display colocalization at the light and ultrastructural microscopic levels (64–68). Such results support the view that NMDARs and opioid receptors display significant interactions, either by direct binding of the receptors or by downstream signaling pathways. Such a scenario, as well as our results, are consistent with there being some level of μOR activity permitting blockade of NMDARs by ketamine or permitting the effects of NMDAR blockade by ketamine. In this way, blocking μOR function with naltrexone would prevent the effects of ketamine on NMDAR function, and could account for the cellular and behavioral effects of this study. Since naltrexone can antagonize more than just the μ-opioid subtype (albeit at lower affinities), antagonists with greater specificity will be necessary to elucidate the requirement of each subtype in behavioral processes.

In conclusion, our study finds that the actions of ketamine are not mimicked by activating μORs, indicating ketamine is not acting as an opioid to produce antidepressive effects in a rodent model. However, the opioid system is required for the actions of ketamine, indicating an interaction between the NMDA receptor and opioid receptor systems.

ACKNOWLEDGMENTS. This work was supported by the National Institute of Mental Health [R.M., R01MH091119; M.E.K., R25MH101072 (principal investigator Neal Swerdlow)]. We thank Dr. Neal Swerdlow for his help with the manuscript and statistical analyses, and Sahil Sheth for his help with the behavioral tasks.

1. P. Zanos *et al.*, Ketamine and ketamine metabolite pharmacology: Insights into therapeutic mechanisms. *Pharmacol. Rev.* **70**, 621–660 (2018).
2. K. A. Lapidus *et al.*, A randomized controlled trial of intranasal ketamine in major depressive disorder. *Biol. Psychiatry* **76**, 970–976 (2014).
3. C. J. Harmer, R. S. Duman, P. J. Cowen, How do antidepressants work? New perspectives for refining future treatment approaches. *Lancet Psychiatry* **4**, 409–418 (2017).
4. B. L. Roth *et al.*, The ketamine analogue methoxetamine and 3- and 4-methoxy analogues of phencyclidine are high affinity and selective ligands for the glutamate NMDA receptor. *PLoS One* **8**, e59334 (2013).
5. B. Ebert, S. Mikkelsen, C. Thorkildsen, F. M. Borgbjerg, Norketamine, the main metabolite of ketamine, is a non-competitive NMDA receptor antagonist in the rat cortex and spinal cord. *Eur. J. Pharmacol.* **333**, 99–104 (1997).
6. N. D. Iadarola *et al.*, Ketamine and other *N*-methyl-D-aspartate receptor antagonists in the treatment of depression: A perspective review. *Ther. Adv. Chronic Dis.* **6**, 97–114 (2015).
7. A. E. Autry *et al.*, NMDA receptor blockade at rest triggers rapid behavioural antidepressant responses. *Nature* **475**, 91–95 (2011).
8. O. Hustveit, A. Maurset, I. Oye, Interaction of the chiral forms of ketamine with opioid, phencyclidine, sigma and muscarinic receptors. *Pharmacol. Toxicol.* **77**, 355–359 (1995).
9. A. Gupta, L. A. Devi, I. Gomes, Potentiation of μ-opioid receptor-mediated signaling by ketamine. *J. Neurochem.* **119**, 294–302 (2011).
10. D.d.F. Pacheco, T. R. Romero, I. D. Duarte, Central antinociception induced by ketamine is mediated by endogenous opioids and μ- and δ-opioid receptors. *Brain Res.* **1562**, 69–75 (2014).
11. S. Ryder, W. L. Way, A. J. Trevor, Comparative pharmacology of the optical isomers of ketamine in mice. *Eur. J. Pharmacol.* **49**, 15–23 (1978).
12. A. D. Finck, S. H. Ngai, Opiate receptor mediation of ketamine analgesia. *Anesthesiology* **56**, 291–297 (1982).
13. E. Sarton *et al.*, The involvement of the mu-opioid receptor in ketamine-induced respiratory depression and antinociception. *Anesth. Analg.* **93**, 1495–1500 (2001).
14. N. R. Williams *et al.*, Attenuation of antidepressant effects of ketamine by opioid receptor antagonism. *Am. J. Psychiatry* **175**, 1205–1215 (2018).

15. N. R. Williams *et al*., Attenuation of antidepressant and antisuicidal effects of ketamine by opioid receptor antagonism. *Mol. Psychiatry* **24**, 1779–1786 (2019).
16. K. Zhang, K. Hashimoto, Lack of opioid system in the antidepressant actions of ketamine. *Biol. Psychiatry* **85**, e25–e27 (2019).
17. G. Yoon, I. L. Petrakis, J. H. Krystal, Association of combined naltrexone and ketamine with depressive symptoms in a case series of patients with depression and alcohol use disorder. *JAMA Psychiatry* **76**, 337–338 (2019).
18. G. Sanacora, Caution against overinterpreting opiate receptor stimulation as mediating antidepressant effects of ketamine. *Am. J. Psychiatry* **176**, 249 (2019).
19. T. Marton, D. E. Barnes, A. Wallace, J. D. Woolley, Concurrent use of buprenorphine, methadone, or naltrexone does not inhibit ketamine's antidepressant activity. *Biol. Psychiatry* **85**, e75–e76 (2019).
20. M. Fava *et al*., Opioid system modulation with buprenorphine/samidorphan combination for major depressive disorder: Two randomized controlled studies. *Mol. Psychiatry*, 10.1038/s41380-018-0284-1 (29 October 2018).
21. P. E. Lutz, B. L. Kieffer, Opioid receptors: Distinct roles in mood disorders. *Trends Neurosci.* **36**, 195–206 (2013).
22. P. L. Tenore, Psychotherapeutic benefits of opioid agonist therapy. *J. Addict. Dis.* **27**, 49–65 (2008).
23. W. A. Carlezon, Jr, A. D. Krystal, Kappa-opioid antagonists for psychiatric disorders: From bench to clinical trials. *Depress. Anxiety* **33**, 895–906 (2016).
24. M. S. George, Is there really nothing new under the sun? Is low-dose ketamine a fast-acting antidepressant simply because it is an opioid? *Am. J. Psychiatry* **175**, 1157–1158 (2018).
25. M. Matsumoto, O. Hikosaka, Lateral habenula as a source of negative reward signals in dopamine neurons. *Nature* **447**, 1111–1115 (2007).
26. C. D. Proulx, O. Hikosaka, R. Malinow, Reward processing by the lateral habenula in normal and depressive behaviors. *Nat. Neurosci.* **17**, 1146–1152 (2014).
27. E. S. Bromberg-Martin, M. Matsumoto, O. Hikosaka, Dopamine in motivational control: Rewarding, aversive, and alerting. *Neuron* **68**, 815–834 (2010).
28. L. J. Boulos, E. Darcq, B. L. Kieffer, Translating the habenula—From rodents to humans. *Biol. Psychiatry* **81**, 296–305 (2017).
29. A. Friedman *et al*., Electrical stimulation of the lateral habenula produces an inhibitory effect on sucrose self-administration. *Neuropharmacology* **60**, 381–387 (2011).
30. A. Tchenio, S. Lecca, K. Valentinova, M. Mameli, Limiting habenular hyperactivity ameliorates maternal separation-driven depressive-like symptoms. *Nat. Commun.* **8**, 1135 (2017).
31. C. Winter, B. Vollmayr, A. Djodari-Irani, J. Klein, A. Sartorius, Pharmacological inhibition of the lateral habenula improves depressive-like behavior in an animal model of treatment resistant depression. *Behav. Brain Res.* **216**, 463–465 (2011).
32. B. Li *et al*., Synaptic potentiation onto habenula neurons in the learned helplessness model of depression. *Nature* **470**, 535–539 (2011).
33. A. Sartorius *et al*., Remission of major depression under deep brain stimulation of the lateral habenula in a therapy-refractory patient. *Biol. Psychiatry* **67**, e9–e11 (2010).
34. P. J. Carlson *et al*., Neural correlates of rapid antidepressant response to ketamine in treatment-resistant unipolar depression: A preliminary positron emission tomography study. *Biol. Psychiatry* **73**, 1213–1221 (2013).
35. Y. Yang *et al*., Ketamine blocks bursting in the lateral habenula to rapidly relieve depression. *Nature* **554**, 317–322 (2018).
36. H. M. Lachman *et al*., Hippocampal neuropeptide Y mRNA is reduced in a strain of learned helpless resistant rats. *Brain Res. Mol. Brain Res.* **14**, 94–100 (1992).
37. B. Vollmayr, F. A. Henn, Learned helplessness in the rat: Improvements in validity and reliability. *Brain Res. Brain Res. Protoc.* **8**, 1–7 (2001).
38. A. Y. Dombrovski, K. Szanto, L. Clark, C. F. Reynolds, G. J. Siegle, Reward signals, attempted suicide, and impulsivity in late-life depression. *JAMA Psychiatry* **70**, 1 (2013).
39. E. Pulcu *et al*., Temporal discounting in major depressive disorder. *Psychol. Med.* **44**, 1825–1834 (2014).
40. S. J. Shabel, C. Wang, B. Monk, S. Aronson, R. Malinow, Stress transforms lateral habenula reward responses into punishment signals. *Proc. Natl. Acad. Sci. U.S.A.* **116**, 12488–12493 (2019).
41. F. A. Henn, B. Vollmayr, Stress models of depression: Forming genetically vulnerable strains. *Neurosci. Biobehav. Rev.* **29**, 799–804 (2005).
42. A. D. Sherman, J. L. Sacquitne, F. Petty, Specificity of the learned helplessness model of depression. *Pharmacol. Biochem. Behav.* **16**, 449–454 (1982).
43. A. Sartorius, M. M. Mahlstedt, B. Vollmayr, F. A. Henn, G. Ende, Elevated spectroscopic glutamate/gamma-amino butyric acid in rats bred for learned helplessness. *Neuroreport* **18**, 1469–1473 (2007).
44. D. Schulz, M. M. Mirrione, F. A. Henn, Cognitive aspects of congenital learned helplessness and its reversal by the monoamine oxidase (MAO)-B inhibitor deprenyl. *Neurobiol. Learn. Mem.* **93**, 291–301 (2010).
45. C. D. Proulx *et al*., A neural pathway controlling motivation to exert effort. *Proc. Natl. Acad. Sci. U.S.A.* **115**, 5792–5797 (2018).
46. C. D. Kopec *et al*., A robust automated method to analyze rodent motion during fear conditioning. *Neuropharmacology* **52**, 228–233 (2007).
47. R. Rygula *et al*., Anhedonia and motivational deficits in rats: Impact of chronic social stress. *Behav. Brain Res.* **162**, 127–134 (2005).
48. K. M. Tye *et al*., Dopamine neurons modulate neural encoding and expression of depression-related behaviour. *Nature* **493**, 537–541 (2013).
49. M. R. Warden *et al*., A prefrontal cortex-brainstem neuronal projection that controls response to behavioural challenge. *Nature* **492**, 428–432 (2012).
50. K. Raynor *et al*., Pharmacological characterization of the cloned kappa-, delta-, and mu-opioid receptors. *Mol. Pharmacol.* **45**, 330–334 (1994).
51. J. D. Salamone *et al*., The pharmacology of effort-related choice behavior: Dopamine, depression, and individual differences. *Behav. Processes* **127**, 3–17 (2016).
52. J. T. Pelton, W. Kazmierski, K. Gulya, H. I. Yamamura, V. J. Hruby, Design and synthesis of conformationally constrained somatostatin analogues with high potency and specificity for mu opioid receptors. *J. Med. Chem.* **29**, 2370–2375 (1986).
53. S. Lecca, F. J. Meye, M. Mameli, The lateral habenula in addiction and depression: An anatomical, synaptic and behavioral overview. *Eur. J. Neurosci.* **39**, 1170–1178 (2014).
54. C. Kraus, B. Kadriu, R. Lanzenberger, C. A. Zarate, Jr, S. Kasper, Prognosis and improved outcomes in major depression: A review. *Transl. Psychiatry* **9**, 127 (2019).
55. E. B. Margolis, H. L. Fields, Mu opioid receptor actions in the lateral habenula. *PLoS One* **11**, e0159097 (2016).
56. L. J. Boulos *et al*., Mu opioid receptors in the medial habenula contribute to naloxone aversion. *Neuropsychopharmacology* **45**, 247–255 (2020).
57. A. E. Mechling *et al*., Deletion of the mu opioid receptor gene in mice reshapes the reward-aversion connectome. *Proc. Natl. Acad. Sci. U.S.A.* **113**, 11603–11608 (2016).
58. J. Mao, NMDA and opioid receptors: Their interactions in antinociception, tolerance and neuroplasticity. *Brain Res. Brain Res. Rev.* **30**, 289–304 (1999).
59. P. Sánchez-Blázquez, M. Rodríguez-Muñoz, E. Berrocoso, J. Garzón, The plasticity of the association between mu-opioid receptor and glutamate ionotropic receptor N in opioid analgesic tolerance and neuropathic pain. *Eur. J. Pharmacol.* **716**, 94–105 (2013).
60. T. Jolas, G. K. Aghajanian, Opioids suppress spontaneous and NMDA-induced inhibitory postsynaptic currents in the dorsal raphe nucleus of the rat in vitro. *Brain Res.* **755**, 229–245 (1997).
61. R. Przewlocki *et al*., Opioid enhancement of calcium oscillations and burst events involving NMDA receptors and L-type calcium channels in cultured hippocampal neurons. *J. Neurosci.* **19**, 9705–9715 (1999).
62. G. Martin, Z. Nie, G. R. Siggins, Mu-opioid receptors modulate NMDA receptor-mediated responses in nucleus accumbens neurons. *J. Neurosci.* **17**, 11–22 (1997).
63. L. M. Kow, K. G. Commons, S. Ogawa, D. W. Pfaff, Potentiation of the excitatory action of NMDA in ventrolateral periaqueductal gray by the mu-opioid receptor agonist, DAMGO. *Brain Res.* **935**, 87–102 (2002).
64. M. J. Glass, L. Vanyo, L. Quimson, V. M. Pickel, Ultrastructural relationship between *N*-methyl-D-aspartate-NR1 receptor subunit and mu-opioid receptor in the mouse central nucleus of the amygdala. *Neuroscience* **163**, 857–867 (2009).
65. M. Narita *et al*., Post-synaptic action of morphine on glutamatergic neuronal transmission related to the descending antinociceptive pathway in the rat thalamus. *J. Neurochem.* **104**, 469–478 (2008).
66. K. G. Commons, E. J. van Bockstaele, D. W. Pfaff, Frequent colocalization of mu opioid and NMDA-type glutamate receptors at postsynaptic sites in periaqueductal gray neurons. *J. Comp. Neurol.* **408**, 549–559 (1999).
67. M. Rodríguez-Muñoz, P. Sánchez-Blázquez, A. Vicente-Sánchez, E. Berrocoso, J. Garzón, The mu-opioid receptor and the NMDA receptor associate in PAG neurons: Implications in pain control. *Neuropsychopharmacology* **37**, 338–349 (2012).
68. M. Rodríguez-Muñoz *et al*., The histidine triad nucleotide-binding protein 1 supports mu-opioid receptor-glutamate NMDA receptor cross-regulation. *Cell. Mol. Life Sci.* **68**, 2933–2949 (2011).